

Synthesis and Structure of Two New Layered Ternary Nitrides, SrZrN₂ and SrHfN₂

D. H. Gregory,^{*,†} M. G. Barker,[†] P. P. Edwards,[‡] and D. J. Siddons[†]

Department of Chemistry, The University of Nottingham, Nottingham NG7 2RD, U.K., and School of Chemistry, University of Birmingham, Edgbaston, Birmingham B15 2TT, U.K.

Received June 26, 1996[⊗]

The new ternary nitrides SrZrN₂ and SrHfN₂ have been synthesized by the solid state reactions of Sr₂N with ZrN and HfN and characterized by powder X-ray diffraction. Both nitrides form structures in the hexagonal space group *R* $\bar{3}m$ (SrZrN₂, *a* = 3.37302(5) Å, *c* = 17.6756(3) Å, *Z* = 3; SrHfN₂, *a* = 3.34481(3) Å, *c* = 17.6779(2) Å, *Z* = 3) and are isostructural with α -NaFeO₂. The structures are constructed of alternating layers of strontium–nitrogen edge-sharing octahedra and either zirconium–nitrogen or hafnium–nitrogen edge-sharing octahedra stacked along the *c* axis. Alternatively, Sr²⁺ can be regarded as occupying octahedral holes between Zr(Hf)N₂ octahedral layers. The title nitrides are essentially diamagnetic at room temperature, consistent with the chemical composition. These compounds are the first alkaline earth ternary nitrides observed to have the α -NaFeO₂ layered structure.

Introduction

There has been much interest in the chemistry of the ternary and higher order transition metal nitrides. Many of these materials have been the subject of speculation regarding their physical properties and potential applications. Preparative routes to ternary nitrides are often practically difficult, and there is no question that this has previously limited work in this field. Several groups have reported new ternary nitride compounds that exhibit a wide range of diverse and often novel crystal structures.^{1–4} In some of these structures, transition metal ions display unusual oxidation states and/or coordination to nitrogen which are often unique to ternary nitride chemistry. For example, the families of ternary phases A₃MN₃ (313)^{5–8} (A = alkaline earth, M = V, Cr, Mn, Fe) and Ca₆MN₅ (615)^{9,10} (M = Fe, Ga, Mn) contain M³⁺ coordinated to three nitrogens and have structures consisting of sheets of carbonate-like [MN₃]⁶⁻ planar triangular units separated by alkaline earth cations. Other nitrides adopt structures seen in carbide and oxide chemistry. For instance, CaNiN has the YCoC structure containing Ni(I) in chains of linear Ni–N units that run perpendicular to the long *c* axis.¹¹ Ba₂VN₃, however, forms the orthorhombic Rb₂TiO₃ structure containing chains of corner-sharing [VN₃]⁴⁻ tetrahedra.¹²

Ternary nitrides of stoichiometry AMN₂ (A = alkali metal, alkaline earth metal, or transition metal; M = transition metal or lanthanide) crystallize in a variety of different structures. This stoichiometry is relatively well-documented for ternary alkali

metal nitrides, and the majority of group 1a transition metal nitrides form layered structures similar to those seen in ternary oxide and chalcogenide chemistry. LiMN₂ (M = Mo, W) are hexagonal layered compounds with Mo or W coordinated to six nitrogens in trigonal prismatic coordination.^{13,14} These nitrides are reported to be paramagnetic and metallic in nature. The alkali metal nitrides ATaN₂ (A = K, Rb, Cs) have structures related to that of β -cristobalite whereas the ternary nitrides NaMN₂ (M = Nb, Ta) have the layered α -NaFeO₂ structure.^{15–17} In the latter materials both cations are coordinated to nitrogen in an octahedral geometry.

Mixed transition metal nitrides such as MnWN₂, CoWN₂, NiWN₂,^{18,19} Fe_{0.8}Mo_{1.2}N₂,²⁰ and FeWN₂²¹ are layered materials similar in structure to LiMoN₂ with alternating layers of A–N octahedra and M–N trigonal prisms. As with LiMoN₂, these materials are metallic and paramagnetic. CuTa₂N₂, however, crystallizes in the α -CuFeO₂-type (delafossite) structure.²²

Alkaline earth ternary nitrides of the AMN₂ stoichiometry are much less well-known. Two structural types have been reported to date and these are also layered materials. BaCeN₂ is isostructural with β -RbScO₂ having Ce(IV) octahedrally coordinated to nitrogen and Ba²⁺ occupying trigonal prismatic holes.²³ Remaining known AMN₂ alkaline earth nitrides are formed with transition metals in group IVa. SrTiN₂ and BaZrN₂ are isostructural and form materials isotypic with KCoO₂ in which the layers consist of edge-sharing Ti–N or Zr–N square-based pyramids.^{24,25} The alkaline earth ions in these compounds

[†] The University of Nottingham.

[‡] The University of Birmingham.

[⊗] Abstract published in *Advance ACS Abstracts*, November 15, 1996.

- Brese, N. E.; O'Keeffe, M. *Struct. Bonding* **1992**, *79*, 307.
- Metselaar, R. *Pure Appl. Chem.* **1994**, *66*, 1815.
- Vennos, D. A.; Badding, M. E.; DiSalvo, F. J. *Inorg. Chem.* **1990**, *29*, 4059.
- Höhn, P.; Kniep, R.; Rabenau, A. *Z. Kristallogr.* **1991**, *196*, 153.
- Vennos, D. A.; DiSalvo, F. J. *J. Solid State Chem.* **1992**, *98*, 318.
- Tennstedt, A.; Röhr, C.; Kniep, R. *Z. Naturforsch.* **1993**, *48B*, 794.
- Tennstedt, A.; Röhr, C.; Kniep, R. *Z. Naturforsch.* **1993**, *48B*, 1831.
- Barker, M. G.; Begley, M. J.; Edwards, P. P.; Gregory, D. H.; Smith, S. E. *J. Chem. Soc., Dalton Trans.* **1996**, *1*.
- Cordier, G.; Höhn, P.; Kniep, R.; Rabenau, A. *Z. Anorg. Allg. Chem.* **1990**, *591*, 58.
- Gregory, D. H.; Barker, M. G.; Edwards, P. P.; Siddons, D. J. *Inorg. Chem.* **1995**, *34*, 5195.
- Chern, M. Y.; DiSalvo, F. J. *J. Solid State Chem.* **1990**, *88*, 459.
- Gregory, D. H.; Barker, M. G.; Edwards, P. P.; Siddons, D. J. *Inorg. Chem.* **1995**, *34*, 3912.

- Elder, S. H.; Doerrer, L. H.; DiSalvo, F. J.; Parise, J. B.; Guyomard, D.; Tarascon, J. M. *Chem. Mater.* **1992**, *4*, 928.
- Herle, P. S.; Hegde, M. S.; Vasanthacharya, N. Y.; Gopalakrishnan, J.; Subbanna, G. N. *J. Solid State Chem.* **1994**, *112*, 208.
- Jacobs, H.; von Pinkowski, E. *J. Less-Common Met.* **1989**, *146*, 147.
- Rauch, P. E.; DiSalvo, F. J. *J. Solid State Chem.* **1992**, *100*, 160.
- Jacobs, H.; Hellmann, B. *J. Alloys Comp.* **1993**, *191*, 51.
- Grins, J.; Käll, P.-O.; Svensson, G. *J. Mater. Chem.* **1995**, *5*, 571.
- Herle, P. S.; Vasanthacharya, N. Y.; Hegde, M. S.; Gopalakrishnan, J. *J. Alloys Comp.* **1995**, *217*, 22.
- Bem, D. S.; Olsen, H. P., zur Loye, H.-C. *Chem. Mater.* **1995**, *7*, 1824.
- Bem, D. S.; zur Loye, H.-C. *J. Solid State Chem.* **1993**, *104*, 467.
- Zachwieja, U.; Jacobs, H. *Eur. J. Solid State Inorg. Chem.* **1991**, *28*, 1055.
- Seeger, O.; Strähle, J. *Z. Naturforsch.* **1994**, *49B*, 1169.
- Gregory, D. H.; Barker, M. G.; Edwards, P. P.; Siddons, D. J. In preparation.
- Seeger, O.; Hoffmann, M.; Strähle, J.; Laval, J. P.; Frit, B. *Z. Anorg. Allg. Chem.* **1994**, *620*, 2008.

are situated between M–N layers level with the apices of the pyramids. Magnetic measurements have been performed on the latter material. Given the nominal stoichiometry, BaZrN₂ shows anomalous magnetic behavior, exhibiting temperature-independent paramagnetism between 20 and 300 K.

As part of comprehensive research into the synthesis, crystal chemistry, and physical properties of ternary transition metal nitrides, we report here the syntheses and structures of two new layered AMN₂ materials, SrZrN₂ and SrHfN₂. These compounds are the first examples of alkaline earth metal nitrides with the α -NaFeO₂ structure, a structure commonly observed in AMO₂ materials.

Experimental Section

Starting Material. The starting material Sr₂N was prepared by the reaction of the molten alkaline earth metal-sodium alloy with dried nitrogen at 520 °C as detailed in the preparation of other ternary strontium nitride phases.^{8,12} Molten alkali and alkaline earth metals are highly reactive to air and water, and these were handled under inert atmospheres at all times. The alloy was made by adding clean Sr metal to molten sodium in a stainless steel crucible at 250 °C in an argon-filled glovebox. The cooled crucible of alloy was contained in a stainless steel vessel and heated to 520 °C under a positive pressure of nitrogen, monitored by a pressure transducer, until the gas pressure remained constant. Excess sodium was removed by heating under vacuum at 400 °C for 24 h. Liquid sodium is unreactive toward nitrogen and serves as an inert solvent for the alkaline earth metals. This method produced strontium nitride (Sr₂N) containing negligible amounts of the alkaline earth oxide. The reaction yielded crystalline samples of purple-black Sr₂N. The identity of Sr₂N was confirmed by powder X-ray diffraction (PXD).

Synthesis of SrZrN₂ and SrHfN₂. Polycrystalline samples of SrZrN₂ and SrHfN₂ were prepared by the high-temperature solid state reaction of the binary alkaline earth nitride and either zirconium nitride (ZrN) (99%) or hafnium nitride (HfN) (99%) powders. All preparations were carried out in a purified argon-filled glovebox. The Sr₂N and ZrN (HfN) powders were thoroughly mixed, ground together in a 1:1 molar ratio, and pelleted using a hand press. The pellets were wrapped in a molybdenum foil tube and placed within stainless steel crucibles which were subsequently welded closed under purified argon. The stainless steel crucibles were fired in a tube furnace at 1000 °C for 5 days under flowing argon to prevent oxidation of the steel and then cooled at 20 °C/h to room temperature, again under flowing argon. The outer surfaces of the cooled crucibles were mechanically cleaned to remove any oxidized steel. The cleaned crucibles were then cut open in a nitrogen-filled glovebox. There was no apparent reaction of the nitrides with the Mo tube, and the resulting powders of SrZrN₂ and SrHfN₂ were both dark gray/green.

Characterization and Structure Determination. PXD data were collected using a Philips XPERT θ – 2θ diffractometer with Cu K α radiation. In each case, the sample was loaded in a nitrogen-filled glovebox onto an aluminum slide contained in an aluminum holder with a Mylar film window and threaded removable cover with O-ring seal. This arrangement allowed powder data of air-sensitive materials to be collected without Mylar peaks appearing in the diffraction pattern. Initially ca. 60 min scans were taken of each sample over a 2θ range of 5–80° to assess sample purity and to determine lattice parameters. Purity was assessed by using the IDENTIFY routine as part of the Philips diffraction software package on a PC which allows access to the JCPDS database. Samples of SrZrN₂ and SrHfN₂ were shown to contain small amounts of SrO and Sr metal. These impurities are to be expected from the starting ratios which generate Sr as an additional product. Each sample also contained small quantities of the respective group IVa binary nitride, ZrN or HfN. The remaining peaks of each pattern were indexed by using a combination of the PC software programs VISSER,²⁶ DICVOL91,^{27,28} and TREOR90.²⁹ Lattice parameters were refined by least-squares fitting of PXD data.

The space group was deduced to be $R\bar{3}m$ by considering the observed reflections and systematic absences. A starting model was obtained by taking the well-documented α -NaFeO₂ structure and substituting Sr, Zr (Hf), and N for Na, Fe-, and O, respectively. A simulated powder pattern was generated using LAZY PULVERIX.³⁰ on a PC using the above model and the refined lattice parameters from the PXD data. A convincing agreement between the calculated and observed patterns was obtained. Diffraction data suitable for Rietveld refinement were collected over the range 5–130° 2θ with step size 0.02° 2θ . Scans were run for approximately 16 h. Full profile Rietveld refinements³¹ of SrZrN₂ and SrHfN₂ were performed using the Philips PC RIETVELD PLUS^{32,33} package with the above α -NaFeO₂-type structures as initial models and with cell parameters obtained from least-squares fitting of PXD data. Peak shapes were modeled using the pseudo-Voigt function, and the background was refined as a polynomial function in each case.

Initial cycles in the refinements of SrZrN₂ and SrHfN₂ allowed for the variation of the scale factor, zero point, background parameters, and lattice parameters. As the refinement progressed, atomic positions and peak width parameters were introduced. In final cycles, isotropic temperature factors were introduced. Attempts to vary temperature factors of atomic sites anisotropically were unsuccessful without a destabilization in the refinement. Variation of the N site isotropic temperature factor in the refinement of SrHfN₂ led to a consistent small negative value being observed. In final cycles this was set to a low positive value, similar in magnitude to the metal site temperature factors, without increasing *R* factors.

Taking into account the anomalous magnetic behavior observed in BaZrN₂ and any possible associated nitrogen nonstoichiometry, variation of the occupancy of the N site was attempted during the refinements of the two strontium nitrides. However, in both cases, varying the N site occupancy led to values above 100%, a corresponding decrease of the isotropic temperature factor, and destabilization of the refinement. The N site occupancy was therefore left fixed at 100%. This is essentially consistent with the observed magnetic data (see below). It is not uncommon for layered AMX₂ phases to exhibit metal site disordering (for example, LiMoN₂ in ternary nitride chemistry¹³), especially when the sizes of A and M are similar. Although, Sr is somewhat larger than Zr or Hf (1.16, 0.72, and 0.71 Å for Sr²⁺, Zr⁴⁺, and Hf⁴⁺, respectively, in 6-fold coordination),³⁴ the possibility was tested in the refinements of the two nitrides. Variation of the site occupancies indicated only a negligible degree of disorder with no decrease in *R* factors and a decrease in temperature factors to the point where either or both of the metal site *B* values fluctuated just above and below zero. The original ordered arrangement was thus retained in the final model.

Impurity phases of SrO, Sr, α -Sr, and ZrN (HfN) were simultaneously refined in each case. Quantitative analysis of the diffraction data running as part of the PC RIETVELD PLUS package yielded weight percentage values of 5.6% SrO, 5.5% Sr, 11.1% α -Sr, and 7.2% ZrN for SrZrN₂ and 14.0% SrO, 2.1% Sr, 4.1% α -Sr, and 2.6% HfN for SrHfN₂, respectively. Observed, calculated, and difference plots for the refinements of SrZrN₂ and SrHfN₂ are shown in Figures 1 and 2.

Magnetic Measurements. Magnetic susceptibility measurements were performed at room temperature using a Johnson Matthey magnetic susceptibility balance. Samples (ca. 0.15 g) of SrZrN₂ and SrHfN₂ were thoroughly ground and loaded into preweighed silica sample tubes in an argon-filled glovebox. Sample tubes were filled to a height of ca. 1.5 cm and sealed. After correction for the diamagnetism of the sample tubes, values for the total mass susceptibility, χ_g , of 3.393×10^{-6} and 1.705×10^{-7} emu g⁻¹ were obtained for SrZrN₂ and SrHfN₂, respectively. The magnetic susceptibilities would appear to suggest intrinsically diamagnetic materials with varying amounts of paramagnetic impurities (either ZrN or HfN, for example) present in each sample.

(26) Visser, J. W. *J. Appl. Crystallogr.* **1969**, *2*, 89.

(27) Louer, D.; Louer, M. *J. Appl. Crystallogr.* **1972**, *5*, 271.

(28) Boulif, A.; Louer, D. *J. Appl. Crystallogr.* **1991**, *24*, 987.

(29) Werner, P. -W. *Z. Kristallogr.* **1964**, *120*, 375.

(30) Yvon, K.; Jeitschko, W.; Parthe, E. *J. Appl. Crystallogr.* **1977**, *10*, 73

(31) Rietveld, H. M. *J. Appl. Crystallogr.* **1969**, *2*, 65.

(32) Wiles, D. B.; Young, R. A. *J. Appl. Crystallogr.* **1981**, *14*, 149.

(33) Howard, C. J.; Hill, R. *J. AEC Rep.* **1986**, No. M112.

(34) Shannon, R. D.; Prewitt, C. T. *Acta Crystallogr.* **1969**, B25, 925.

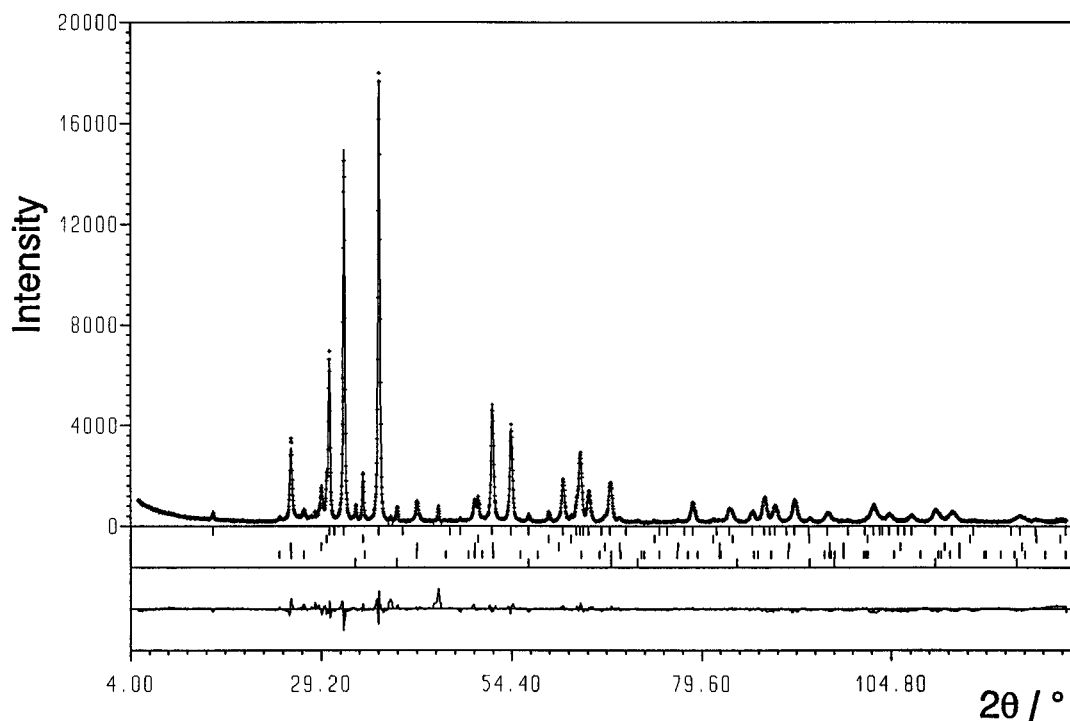


Figure 1. Observed, calculated, and difference plots for SrZrN₂.

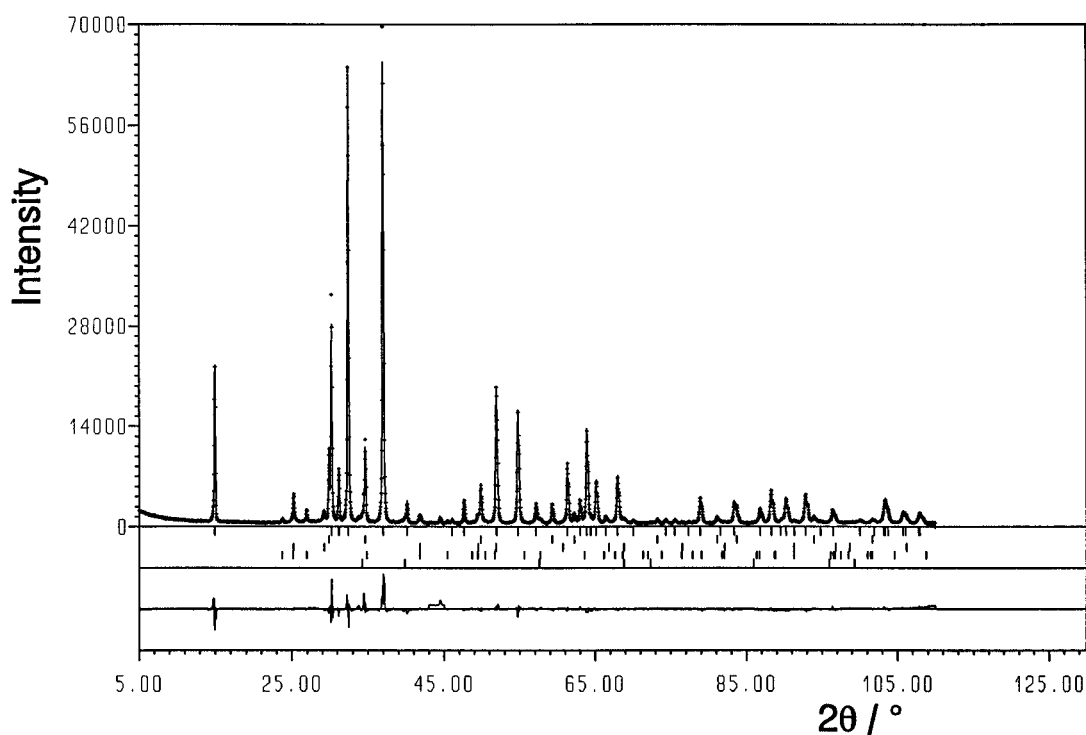


Figure 2. Observed, calculated, and difference plots for SrHfN₂.

Results and Discussion

The final crystallographic results for SrZrN₂ and SrHfN₂ are shown in Table 1. SrZrN₂ and SrHfN₂ are isostructural with each other and are isotypic with α -NaFeO₂. The structure is made up of [ZrN₂]²⁻ or [HfN₂]²⁻ anions and Sr²⁺ cations and is a rhombohedral distortion of the NaCl structure type brought about by the ordering of the A and M cations. The octahedral [MN₂]²⁻ (M = Zr, Hf) anions are linked by edges in the *ab* plane to form layers separated by Sr²⁺ cations in octahedral holes (Figure 3). Thus alternating Zr (Hf)-N and Sr-N octahedral layers create infinite sheets stacked along the *c* axis. Sheet oxide materials can be classified according to their packing

and cation coordination.³⁵ The zirconium and hafnium layered nitrides can be classified by analogy as so-called O3 structures where O refers to the octahedral coordination of the A cation and 3 refers to the number of [MX₂]_n (X = O, S, or N in this instance) sheets present in the unit cell. The nitrogen layer packing follows a repeat pattern of ABCABC. Important interatomic distances and bond angles around the metal and nitrogen atoms in SrZrN₂ and SrHfN₂ are shown in Table 2.

The octahedral Zr-N and Hf-N anions are composed of the group IVa metals coordinated to six equidistant nitrogens at

(35) Delmas, C.; Braconnier, J. J.; Fouassier, C.; Hagenmuller, P. Z. *Naturforsch.* **1996**, *36B*, 1368.

Table 1. Crystallographic Data for SrZrN₂ and SrHfN₂

	SrZrN ₂	SrHfN ₂
space group	$R\bar{3}m$	$R\bar{3}m$
<i>a</i> /Å	3.37302(5)	3.34481(3)
<i>c</i> /Å	17.6756(3)	17.6779(2)
atom (site)		
Sr (3a)		
<i>x</i>	0	0
<i>y</i>	0	0
<i>z</i>	0	0
<i>B</i> ^a	0.33(4)	0.03(2)
Zr/Hf (3b)		
<i>x</i>	0	0
<i>y</i>	0	0
<i>z</i>	0.5	0.5
<i>B</i> ^a	0.21(4)	0.05(2)
N (6c)		
<i>x</i>	0	0
<i>y</i>	0	0
<i>z</i>	0.2350(2)	0.2346(3)
<i>B</i> ^a	0.24(9)	0.02
<i>R</i> ₁ /%	1.10	1.97
<i>R</i> _p /%	5.43	5.17
<i>R</i> _w _p /%	7.38	7.64
<i>R</i> _c /%	1.41	0.78

^a Where $B = \frac{4}{3}[a^2B_{11} + b^2B_{22} + c^2B_{33} + ab(\cos \gamma)B_{12} + ac(\cos \beta)B_{13} + bc(\cos \alpha)B_{23}]$.

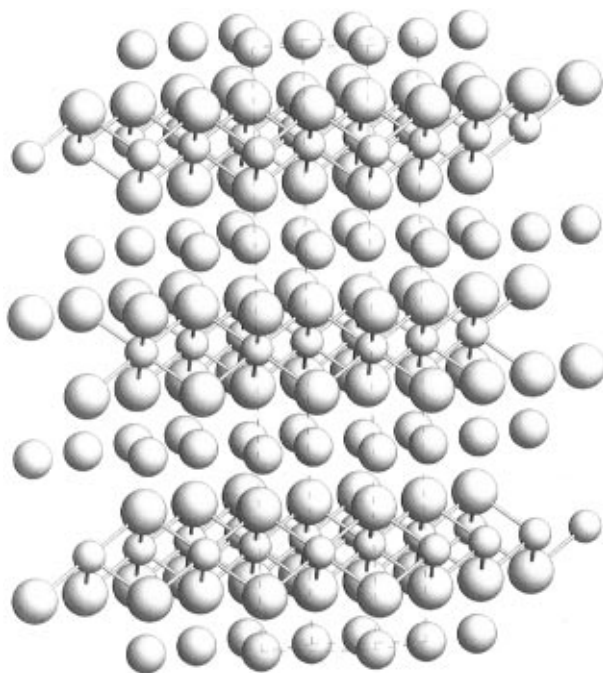


Figure 3. Structure of SrZrN₂ (SrHfN₂) viewed perpendicular to the long *c* axis. The unit cell is indicated by the dashed lines. Large spheres represent nitrogen atoms, medium spheres represent strontium atoms, and small spheres represent zirconium (hafnium) atoms.

2.292(2) and 2.273(2) Å for SrZrN₂ and SrHfN₂, respectively. There is some distortion with N–Zr(Hf)–N angles deviating significantly from 90° (six N–Zr(Hf)–N angles of ca. 95°, six N–Zr(Hf)–N angles of ca. 85°). As might be expected from the relatively small difference in ionic radius for Zr⁴⁺ and Hf⁴⁺ (0.72 and 0.71 Å, respectively³⁴), there is no great disparity in the M–N bond lengths in the respective M–N anions. This is reflected in the overall structures where the *a* and *c* parameters are close in value and the cell volumes are very similar in size (~174 and ~171 Å³ for SrZrN₂ and SrHfN₂, respectively).

The metal–nitrogen distances compare well to those seen in binary phases of zirconium and hafnium with nitrogen. The Zr–N distance in ZrN is 2.292(1) Å³⁶ whereas the mean Hf–N

Table 2. Selected Bond Lengths and Angles in SrZrN₂ and SrHfN₂

SrZrN ₂			
Sr–N/Å	N–Sr–N/deg	Sr–N–Sr/deg	Sr–N–Zr/deg
2.609(3) × 6	180.0(1) × 3 99.48(8) × 6 80.52(8) × 6	80.518(6) × 2	170.06(1) × 3 91.929(1) × 4 91.935(1) × 2
Zr–N/Å	N–Zr–N/deg	Zr–N–Zr/deg	
2.292(2) × 6	180.0(1) × 3 94.79(9) × 4 94.78(9) × 2 85.20(9) × 4 85.21(9) × 2	94.791(7) × 2 94.785(7)	
SrHfN ₂			
Sr–N/Å	N–Sr–N/deg	Sr–N–Sr/deg	Sr–N–Hf/deg
2.602(3) × 6	180.0(1) × 3 100.01(9) × 4 100.02(9) × 2 79.98(9) × 6	79.984(7) × 2 79.980(7)	169.78(1) × 3 92.226(2) × 4 92.231(2) × 2
Hf–N/Å	N–Hf–N/deg	Hf–N–Hf/deg	
2.273(2) × 6	180.0(1) × 3 94.7(1) × 6 85.3(1) × 6	94.689(9) × 2 94.682(9)	

distances are 2.258 Å in Hf₃N₂ and 2.263 Å in Hf₄N₃.³⁷ The only reported ternary alkali metal or alkaline earth metal zirconium or hafnium nitrides are Li₂ZrN₂, Li₂HfN₂,^{38–40} and BaZrN₂.²⁵ The lithium zirconium nitride was characterized recently by powder neutron diffraction.⁴⁰ Zirconium is coordinated to nitrogen in a regular octahedral geometry with a Zr–N bond distance of 2.253(2) Å. This distance is shorter than that observed in SrZrN₂. The mean Zr–N distance of 2.16(1) Å in BaZrN₂,²⁵ where Zr is in a square-based pyramidal coordination to N, is shorter still. The discrepancy in bond distances may be indicative of the degree of multiple Zr–N bonding in the nitrides but may also suggest a small degree of Sr/Zr disordering over the two metal sites in SrZrN₂.

The nearly identical strontium–nitrogen distances in the compounds (2.609(3) and 2.602(3) Å in the zirconium and hafnium nitrides, respectively) are quite short when compared to those observed in other strontium ternary nitrides. Again, this may imply a low level of Sr/Zr(Hf) site disorder. Sr–N bond lengths are typically of the order of ~2.7 Å in ternary nitrides. For example, mean Sr–N bond lengths of 2.723(9), 2.739(1), and 2.798(11) Å are found in Sr₃MnN₃,⁶ Sr₃CrN₃,⁸ and Sr₂VN₃,¹² respectively. The Sr–N distances in SrZrN₂ and SrHfN₂ are more on a par with the mean Sr–N distance observed in the binary nitride Sr₂N (2.6118(3) Å).⁴¹

It is worth noting at this point, however, the structural similarities between the two SrMN₂ (M = Zr, Hf) nitrides and Sr₂N. The latter has the *anti*-CdCl₂ structure. This is essentially an *anti*-α-NaFeO₂ structure with the (0, 0, 1/2) (M) site vacant. Hence, although the N and Sr sites are interchanged in SrMN₂ (M = Zr, Hf) and Sr₂N, the Sr–N coordination environment is very similar. The octahedral arrangement of nitrogen around strontium in Sr₂N is also distorted in the equatorial plane, with supplementary Sr–N–Sr angles 84.83(2) and 95.17(2)°. The equivalent N–Sr–N angles in SrZrN₂ and SrHfN₂ are ap-

(36) Christensen, A. N. *Acta Chem. Scand.* **1975**, A29, 563.

(37) Rudy, E. *Metall. Trans.* **1970**, 1, 1249.

(38) Palisaar, A. P.; Juza, R. Z. *Anorg. Allg. Chem.* **1971**, 384, 1.

(39) Barker, M. G.; Alexander, I. C. *J. Chem. Soc., Dalton Trans.* **1974**, 2166.

(40) Niewa, R.; Jacobs, H.; Mayer, H. M. Z. *Kristallogr.* **1995**, 210, 513.

(41) Brese, N. E.; O'Keeffe, M. *J. Solid State Chem.* **1990**, 87, 134.

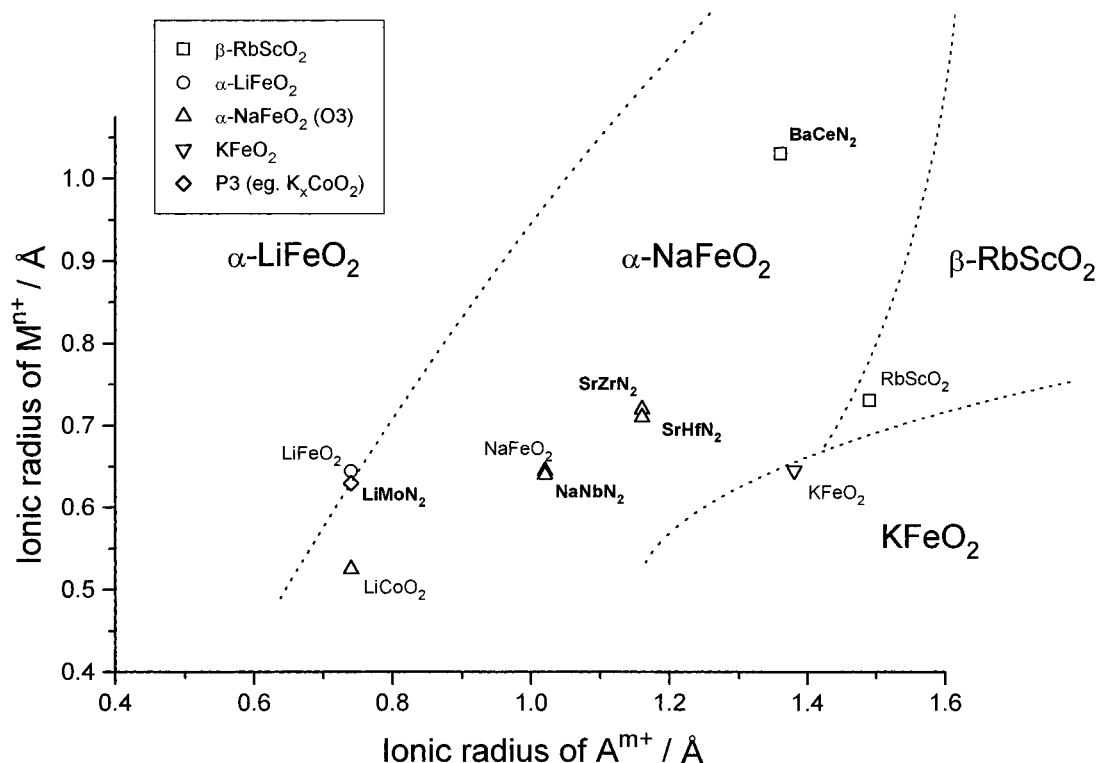


Figure 4. Plot of ionic radius of M against ionic radius of A in selected AMX_2 ($X = O, N$) compounds. Dashed lines show approximate phase boundaries according to ref 44. Ionic radii are taken from ref 34.

proximately 80 and 100°. This increased octahedral distortion, coupled with slightly shorter Sr–N bond lengths, leads to reduced (Sr–N) layer thicknesses in $SrZrN_2$ (~2.41 Å) and $SrHfN_2$ (~2.40 Å) compared to Sr_2N (2.73 Å). The interlayer distances in $SrZrN_2$ and $SrHfN_2$ are 3.476(6) and 3.489(11) Å. As might be expected, these distances are considerably shorter than the equivalent distance between N–Sr layers in Sr_2N (4.17 Å) reflecting the electrostatic repulsion between Sr layers in the latter material.

Nitrogen is coordinated to three strontium atoms and three zirconium (or hafnium) atoms in a distorted octahedral geometry. The octahedron is elongated toward the plane of three Sr atoms. The octahedron is “stretched” along z toward the Sr atoms (three Sr–N–Sr angles of ~80.5°) and compressed along z in the direction of the Zr (Hf) atoms (three Zr–N–Zr angles of ~94.8°).

Bond-valence calculations were performed for the two ternary nitrides using the bond-length parameters proposed by Brese and O’Keeffe for compounds with anions other than oxygen, fluorine, or chlorine.^{42,43} The bond valence parameters used for Sr–N, Zr–N, and Hf–N were 2.23, 2.11, and 2.09 Å, respectively. The calculations resulted in Sr, M, N site valences of 2.15(2), 3.68(2), 2.92(2) and 2.19(2), 3.65(2), 2.93(2) in $SrZrN_2$ and $SrHfN_2$, respectively. The bonding environment changes little by replacing Zr^{4+} by Hf^{4+} , as might be expected from size arguments. In each case, the site valences for Zr or Hf and N are low whereas the site valence for Sr is high.

These results are unusual in the sense that alkaline earth metal valences are commonly lower than expected in binary and ternary nitrides whereas transition metal oxidation states are often higher than expected. Anomalous values for calculated valences are a reflection of shorter or longer than expected metal–nitrogen bonds or unexpected formal oxidation states. In the case of alkaline earth metals, it has been suggested that low values are a consequence of a lower oxidation state rather than longer than anticipated metal–nitrogen bond lengths. For example, in Sr_2N , the nominal stoichiometry implies an oxida-

tion state of 1.5 and bond-valence calculations from neutron diffraction data yield a calculated valence of 1.224;⁴¹ both values are well below the anticipated +2 state.

Conversely, transition metal valences are typically higher than expected in ternary nitrides as a result of shorter than anticipated bond distances. This is assumed to be a factor of multiple metal–nitrogen bonding. In these instances, the bond-valence parameters (which assume essentially ionic, or at least σ , bonds) are too large. For example, in the nitridochromates Ca_3CrN_3 ,³ Sr_3CrN_3 ,⁸ and Ba_3CrN_3 ,⁸ the calculated chromium oxidation states are 3.47(7), 4.17(3), and 4.1(1), respectively.

That these trends are not observed in $SrZrN_2$ and $SrHfN_2$ perhaps suggests two things: first, that the transition metal–nitrogen bonding is essentially σ type (with bond lengths similar to those seen in the equivalent binary nitrides) and, second, that there is some degree of metal site disorder—consequently A–N bonds are on average shorter and M–N bonds are on average longer than might be envisaged. Bond-valence sums calculated from the crystallographic data for the other known ternary nitrido-zirconates indicate a varying degree of multiple Zr–N bonding. In $BaZrN_2$,²⁵ the Zr site valence is large, 4.4(1) as opposed to a value of 4.07(2) in Li_2ZrN_2 .

The structures of the layered oxides, AMO_2 , are well elucidated and have been characterized and classified in terms of ionic radii, interlayer separation, and ionicity.^{35,44} As yet, the number of known AMN_2 ternary nitrides is comparatively small, but on the basis of ionic radii, some of the same general structural trends would seem to apply (Figure 4). For example, if the ionic radii of Sr^{2+} , Zr^{4+} , Hf^{4+} in a six-coordinate environment³⁴ are considered (assuming the relative values of the radii to be essentially unchanged in nitrides compared to oxides), $SrZrN_2$ and $SrHfN_2$ would be expected to lie in the

(42) Brese, N. E.; O’Keeffe, M. *J. Am. Chem. Soc.* **1991**, *113*, 3226.

(43) Brese, N. E.; O’Keeffe, M. *Acta Crystallogr.* **1991**, *B47*, 192.

(44) Delmas, C.; Fouassier, C.; Hagenmuller, P. *Mater. Res. Bull.* **1976**, *11*, 1483.

α -NaFeO₂ region of the M^{n+} ($n = 3, 4, 5$) vs A^{m+} ($m = 1, 2$) graph. NaNbN₂, shown to crystallize with the α -NaFeO₂ (O3) structure,¹⁷ would also lie in this region. LiMoN₂, however, which forms the P3 structure (where P denotes trigonal prismatic A coordination) adopted by nonstoichiometric phases such as K_xCoO₂ ($x < 1$), is placed just within the α -LiFeO₂ region close to the α -NaFeO₂ boundary. Similarly, BaCeN₂, with the β -RbScO₂ structure, is not situated within the β -RbScO₂ region as might be expected, but is found within the α -NaFeO₂ section of the graph. These inconsistencies perhaps highlight the differences in the nature of the bonding between some nitrides and oxides of the same stoichiometry. In this respect, a structure map taking into account metal–anion bond distances is probably more useful than one based purely on “ionic” radii.

The room-temperature magnetic susceptibility measurements carried out on samples of SrZrN₂ and SrHfN₂ are inconclusive. For materials of the nominal stoichiometry AMN₂ (where A is divalent), one would expect M to be in a +4 oxidation state. In the case of Zr⁴⁺ and Hf⁴⁺ (d^0 , $s = 0$), one might also expect a diamagnetic response at room temperature. The presence of ZrN (ca. 8 wt %) and HfN (ca. 3 wt %) in the respective ternary nitrides clearly affects the magnetic measurements. Both of these binary nitride phases are paramagnetic at room temperature and superconducting at low temperature ($T_c = 10.0$ and 8.83

K, respectively).⁴⁵ For the ternary phases not to exhibit intrinsic diamagnetism, vacancies would have to be created in the lattice. Any extent of vacancies on the metal sites would lead to improbably high transition metal oxidation states. Reduction of the nitrogen site population would decrease the M valence (and increase the d electron configuration), but no evidence of this is seen in the structural refinement. Certainly, in oxide chemistry this structure type is most favorable when the A cation stoichiometry is close to 1 and no anion vacancies are observed. Furthermore, no cation or anion vacancies are observed in the structure of NaNbN₂.¹⁷ However, powder X-ray diffraction is limited in its ability to accurately detect small vacancy levels of light elements, and we hope to be performing powder neutron diffraction experiments on the nitrides in the near future.

Acknowledgment. We thank the EPSRC for a postdoctoral fellowship (D.H.G.) and for financial support of this work.

Supporting Information Available: Listings of X-ray diffraction data, including d spacings, observed and calculated intensities, and indexed reflections, and the final cycles in the refinements of SrZrN₂ and SrHfN₂ showing final crystallographic parameters and esd's (24 pages). Ordering information is given on any current masthead page.

IC9607649

(45) Toth, L. E. *Transition Metal Carbides and Nitrides*; Academic Press: New York, 1971.